Multipath Mitigation of 5G Signals via Reinforcement Learning for Navigation in Urban Environments

Ali A. Abdallah[1], Mohamad Orabi[1], and Zaher M. Kassas[1,2]
[1]Department of Electrical Engineering and Computer Science, University of California, Irvine, USA
[2]Department of Mechanical and Aerospace Engineering, University of California, Irvine, USA
Emails: abdalla2@uci.edu, orabim@uci.edu, zkassas@ieee.org

***Abstract*—The ability of reinforcement learning (RL)-based convolutional neural network (CNN) to mitigate multipath signals for opportunistic navigation with downlink 5G signals is assessed. The CNN uses inputs from the autocorrelation function (ACF) to learn the errors in the code phase estimates. A ray tracing algorithm is used to produce high fidelity training data that could model the dynamics between the line of sight (LOS) component and the non-line of sight (NLOS) components. Experimental results on a ground vehicle navigating with 5G signals for 902 m in a multipath-rich environment are presented, demonstrating that the proposed RL-CNN achieved a position root-mean squared error (RMSE) of 14.7 m compared to 20.6 m with a conventional delay-locked loop (DLL).**

***Index Terms*— 5G, reinforcement learning, multipath, navigation.**

I. Introduction

Multipath phenomenon is a major error source in signal-based navigation technologies including: (i) global navigation satellite systems (GNSS) [1] and (ii) alternative technologies, such as cellular, AM/FM radio, satellite communication, digital television, and Wi-Fi [2]–[11]. Among alternative signal-based technologies, cellular 5G signals are particularly attractive due to their ubiquity, geometric diversity, high received signal power, and large bandwidth [12]–[14].

The positioning capabilities of 5G systems have been studied over the past few years. Different approaches have been proposed, in which direction-of-arrival (DOA), direction-of-departure (DOD), time-of-arrival (TOA), or combination thereof is used to achieve accurate positioning from 5G signals. The study in [15] derived the Cramér-Rao lower bound on position and orientation estimation uncertainty and presented an algorithm that achieves the bound for average to high signal-to-noise ratio. In [16], the capability of massive multiple-input multiple-output (mMIMO) systems in providing very accurate localization when relying on DOA was studied. The work in [17] presented an algorithm to mitigate the near-field errors in angular positioning with 5G system. A compressed sensing approach was proposed to address the limitations of DOA in mMIMO systems in the presence of multipath, showing the potential of achieving submeter accuracy in a simulated environment. In contrast to the aforementioned approaches, [18]–[20] were the first to present experimental navigation results on ground and aerial vehicles, achieving meter-level accuracy.

Several techniques have been developed to mitigate the effect of multipath in GNSS systems, most of which could be grouped into three main categories: (i) antenna techniques [21], (ii) signal processing techniques, such as the narrow correlator [22], strobe edge correlator [23], and high resolution correlator (HRC) [24], and (iii) a combination thereof [25]. While the aforementioned approaches have been shown to outperform the standard early-minus-late (E-L) delay-locked loop (DLL), they are still susceptible to severe multipath. Moreover, while signal processing techniques could be extended to receivers that exploit cellular signals opportunistically for navigation, antenna techniques that mitigate multipath by filtering out signals with lower elevation angles are not useful, since most received signals from terrestrial 5G base stations (referred to as gNBs) have low elevation angles.

Machine learning algorithms have found their way into the navigation field [26]. A neural network (NN)-based DLL (NNDLL) was proposed in [27] for multipath mitigation in GPS receivers. The type of multipath environment and receiver motion was identified via an NN in [28] in order to adjust the receiver's tracking strategy. The ability of different NNs to mitigate multipath signals for opportunistic navigation with downlink 5G signals was considered in [29]. The paper presented two NN designs, namely feed-forward NNs (FFNNs) and time-delay NNs (TDNNs), to learn multipath-induced errors on a 5G receiver's code phase estimate. Experimental results in a multipath-rich environment were presented demonstrating that the proposed TDNN achieved ranging root-mean squared error (RMSE) reduction of 27.1% compared to a conventional DLL. However, such NNs are limited due to the dependence on DLL for training data; hence, the NN only corrects the DLL estimates. This paper addresses this limitation by proposing a reinforcement learning (RL)-based approach to learn multipath errors that corrupt the TOA estimate in a 5G opportunistic navigation receiver. The proposed RLNN seeks to learn the multipath behavior by making a sequence of decisions, each with a certain reward and penalty.

This paper assesses the ability of RL-based convolutional NN (CNN) to mitigate multipath signals for opportunistic navigation with downlink 5G signals. The NNs use inputs

from the autocorrelation function (ACF) to learn the errors in the code phase estimate of a conventional DLL. A ray tracing algorithm is used to produce high fidelity training data that could model the dynamics between the line of sight (LOS) component and the non-line of sight (NLOS) components. Experimental results on a ground vehicle navigating in an urban environment are presented demonstrating that the proposed RL-CNN achieved a position root-mean squared error (RMSE) of 14.7 m compared to 20.6 m with a conventional DLL.

This paper is organized as follows. Section II introduces the structure of 5G signals and models the synchronization signals being exploited for navigation. Section III presents the proposed RL-based multipath mitigation approach along with the simulator that was used to generate the training and testing data. Section V presents experimental results in an urban environment. Section VI gives concluding remarks.

II. 5G Signal Structure

This section discusses the 5G signal structure and provides a model for 5G reference signals that can be exploited for opportunistic navigation.

A. 5G Frame Structure

5G systems implement orthogonal frequency-division multiplexing (OFDM) with an adaptive subcarrier spacing $\Delta f = 2^{\mu} \times 15$ kHz, where $\mu \in \{0, 1, 2, 3, 4\}$ is defined as the numerology. 5G is designed to support transmission at different frequency ranges (from 450 MHz to 52.6 GHz). In the time-domain, 5G signals are transmitted in frames of duration $T_f = 10$ ms, which are divided into 10 subframes with a duration of 1 ms each. Subframes are then further divided into 2^{μ} time slots which contain 14 OFDM symbols each of duration $T_{\text{symb}} = \frac{1}{\Delta f}$. In the frequency domain, subframes are divided into a number of resource grids consisting of resource blocks with 12 subcarriers each. The number of resource grids in a frame is determined by higher level parameters. Moreover, a resource element defines the smallest unit of the resource grid spanning a duration of one OFDM symbol and a bandwidth of one subcarrier.

5G systems utilize two maximal-length synchronization signals (SS) of length $N_{\text{SS}} = 127$, known as the primary synchronization signal (PSS) and secondary synchronization signal (SSS) to enable cell search and synchronization at the user equipment (UE). There is a total of three possible PSS sequences, each mapped to an integer representing the sector ID of the gNB denoted by $N_{\text{ID}}^{(2)}$. On the other hand, the SSS is one of 336 possible sequences, each mapped to an integer representing the gNB's group identifier denoted by $N_{\text{ID}}^{(1)}$. This results in a total of 1008 cell identifiers denoted by $N_{\text{ID}}^{\text{cell}} = 3N_{\text{ID}}^{(1)} + N_{\text{ID}}^{(2)}$.

The SS are transmitted along with the physical broadcast channel (PBCH) signal and its associated demodulation reference signal (DM-RS) on a block known as the SS/PBCH block, which spans 20 resource blocks (i.e., 240 subcarriers) and four consecutive OFDM symbols. The SS/PBCH is transmitted numerous times, where each set of these transmitted block is called an SS/PBCH burst. However, each SS/PBCH block in the burst is beamformed in a different direction with a periodicity that can be 5 ms, 10 ms, 20 ms, 40 ms, 80 ms or 160 ms.

B. Signal Model

For the purpose of opportunistic navigation with 5G, the signals of interest for a given $N_{\text{ID}}^{\text{cell}}$ could be modeled as

$$s_{\text{SS}}(t) = \begin{cases} \text{IFT}\{S_{\text{PSS}}(f)\}, & \text{for } t \in (0, T_{\text{symb}}) \\ \text{IFT}\{S_{\text{SSS}}(f)\}, & \text{for } t \in (2T_{\text{symb}}, 3T_{\text{symb}}) \\ 0, & \text{otherwise,} \end{cases}$$

where $S_{\text{PSS}}(f)$ and $S_{\text{SSS}}(f)$ are the frequency-domain representations of the PSS and SSS, respectively. A navigation receiver correlates the replicated SS signal with the received signal, forming the autocorrelation function (ACF), denoted by $R(\tau)$ according to

$$\begin{aligned} R(\tau) &\triangleq y(t) \circledast s_{\text{SS}}(t) \\ &= \text{IFFT}\{Y(f)S_{\text{SS}}^{*}(f)\} \quad (1) \\ &= \text{sinc}\,(B\tau) \quad (2) \end{aligned}$$

where the symbols $\circledast$ and * denote the circular correlation and the complex conjugate operators, respectively, IFFT denotes the inverse fast Fourier transform, and $y(t)$ and $Y(f)$ are the time- and frequency-domain representations of the received signal with a bandwidth of $B = N_{\text{subcarriers}} \cdot \Delta f$, where $N_{\text{subcarriers}}$ is the number of subcarriers allocated for the synchronization signal. Since each symbol of the SS is mapped onto one subcarrier, then $N_{\text{subcarriers}} = N_{\text{SS}} = 127$. It is important to note that while the ACF has a triangular shape for GPS signals, the ACF produced by the correlator of an opportunistic receiver exploiting 5G signals has the shape of the sinc function. This follows from the OFDM modulation of the two maximal-length sequences (m-sequences) PSS and SSS. Equation (2) follows from (1) since $S_{\text{SS}}(f)$ is an m-sequence that takes the values $\{-1, +1\}$, and $S_{\text{SS}}(f)S_{\text{SS}}^{*}(f) = |S_{\text{SS}}(f)|^2 = \text{rect}(\frac{f}{B})$, where rect(.) denotes the standard rectangular function with a bandwidth of B.

III. Proposed Approach

RL is a machine learning technique that seeks modeling a certain environment following the cut-and-try approach. The trained model is denoted by an agent that evaluates a current situation (state). The agent takes a sequence of actions, each receives a feedback (reward/penalty) from an environment. The environment represents the training data to which the agent is making actions. Positive feedback represents a reward for making a correct decision, while negative feedback represents a penalty for making the wrong decision. In other words, RL learns the best action via a trail-and-error approach while interacting with an environment to maximize a long-term reward. The long-term reward is a combination of short-term rewards that are observed in every state after taking a set of coherent actions while interacting with the environment. A block diagram depicting RL is hown in Fig. 1

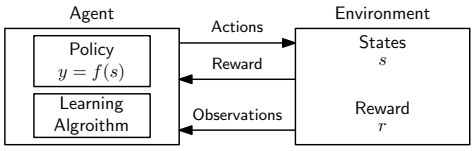

Fig. 1. RL block diagram.

The proposed RL approach consists of the following

- Environment: represents the physical environment on which the agent operates. In particular, it is represented via the ACF $R(\tau)$ that captures all rays impinging on the receiver's antenna including both LOS and NLOS components and the receiver's states.
- State: represents the current situation of the agent. As such, the code phase error is an informative state of the agent while seeking to maintain tracking in presence of multipath.
- Reward: represents the feedback from the environment to evaluate the agent's performance. Here, a potential choice of the reward function r_t is chosen to penalize the code phase error and its first order derivative according to

$$r_t = -|\tilde{\tau}| - \frac{d|\tilde{\tau}|}{dt}, \qquad (3)$$
$$\tilde{\tau} \triangleq \tau_k - \hat{\tau}_k,$$

  where τ, $\hat{\tau}$, $\tilde{\tau}$ are the actual code phase, estimated code phase, and code phase error, respectively. The reward in (3) represents the short-term reward. In addition to that, a milestone reward for surviving five seconds is applied, where surviving inhere denotes $\tilde{\tau} < \frac{B}{4}$, where B is bandwidth of the received 5G signals. Exceeding this bound results in killing the agent and starting another episode. It is worth mentioning that this long-term reward helps with the initial convergence as it helps in filtering out the agents that are immediately killed and gives the agent a push to the right decision.
- Policy: maps the agent's state s to actions $y = f(s)$. To do so, an NN is implemented to decide the actions to be taken. For the proposed approach, a CNN with sixteen 21×3 filters, with a stride of 21×1 were designed. The CNN has 42,757 learnable parameters. Note that "21" represents the number of ACF taps used with 10 delay taps, which are the user's design choices. Fig. 2 shows the proposed RL network design. It worth mentioning that the input is 42×10 instead of 21×10 due to the fact that the real and imaginary parts of each sample point are fed separately to the network.

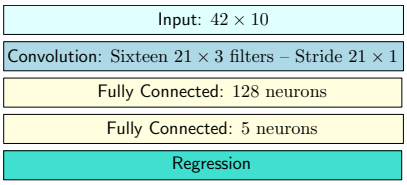

Fig. 2. RL network design.

IV. Training and Data Generation

To simulate a realistic environment, map and terrain data were obtained through OpenStreetMap [30] and Global Multiresolution Terrain Elevation Data (GMTED) [31] for the area around Aldrich Park at the University of California, Irvine (UCI). An opportunistic 5G receiver was then simulated to be moving around the park at a walking speed of 2 m/s. The simulated environment and trajectory are presented in Fig. 3(a). Moreover, the location of the simulated gNB correspond to real gNB positions on top of the Engineering Tower at UCI. The power, delay, and phase of each path were then computed for the entire trajectory using the ray tracing methods available through MATLAB's RadioFrequency (RF) toolbox [32]. The channel impulse response (CIR) was generated in this manner to ensure that the simulator would capture the dynamics between the LOS and NLOS components. Fig. 3(b) shows the simulation environment in MATLAB with the rays traced from the gNB to four sample points within the trajectory along with the received power for each path. It is worth noting that the material used for buildings was concrete with a relative permittivity of 5.31 and a conductivity of 0.0548 Siemens per meter. These values were chosen according to the international telecommunication union (ITU) recommendations, which provide methods, equations, and values used to calculate real relative permittivity, conductivity, and complex relative permittivity for common materials [33].

(a)

(b)

Fig. 3. (a) Receiver Trajectory around Aldirch Park. (b) Rays traced from transmitter (red) to sample points of trajectory (blue).

Next, the obtained CIRs are used to simulate the tracking results for an opportunistic 5G receiver traversing the aforementioned trajectory shown in Fig. 3(a). The tracking loops of the receiver uses inputs from the output of the correlator $R(\tau)$, which is simulated from the CIR according to

$$R_k(\tau) = \sum_{i=1}^{N_k^{\text{paths}}} \alpha_k^i R(\tau - \tau_k^i),$$

where k is the time index with a duration equivalent to that of the SS (set to 20 ms based on an observation of a real 5G transmission scenario), $R_k(\tau)$ is the correlator output of the opportunistic receiver accounting for the different traversed paths at the k-th time-step, $R(.)$ is the ACF of the synchronization signal defined in (2), N_k^{paths} is the total number of paths traversed by the signal, $\alpha_k^i \in \mathcal{C}$ is a complex number representing the power and phase of the signal component corresponding to the i-th path, and τ_k^i represents its delay (time of flight).

Finally, the simulated data contained samples (x_k, y_k) with an equivalent duration of 438.51 seconds. The input $x_k \in \mathcal{C}^{2N_x+1}$ is formed of $2N_x + 1$ samples of the correlator output at the k-th time-step centered around the DLL's code phase estimate, such that $x_k = [x_k^{-N_x}, \ldots, x_k^{N_x}]^\mathsf{T}$, where $x_k^d = R_k(\tau + \hat{\tau}_k^{\mathrm{DLL}} + d/f_s)$ and f_s is the frequency at which the ACF was sampled. For the remainder of this paper, the sampling frequency is set to $f_s \triangleq 4B = 7.62$, and the number of ACF taps used as inputs is $2N_x+1 = 11$. The sample target points $y_k \in \mathcal{R}$ are the errors incurred by the DLL estimate $e(x_k) = \tau_k^{\mathrm{LOS}} - \hat{\tau}_k^{\mathrm{DLL}}$, where the true LOS delays at the k-th time-step τ_k^{LOS} are obtained from the simulated CIR.

V. Experimental Results

This section validates the proposed framrwork on a ground vehicle in an urban environment.

A. Experimental Setup and Environmental Layout

The experiment was performed on the Fairview road in Costa Mesa, California, USA. A quad-channel National Instrument (NI) universal software radio peripheral (USRP)-2955 was mounted on a vehicle, where two channels were used to sample 5G signals with a sampling ratio of 10 MSps. The receiver was equipped with two consumer-grade cellular omnidirectional Laird antennas. The USRP was tuned to listen to 5G signals from AT&T and T-Mobile U.S. cellular providers (see Table I). The vehicle was equipped with a Septentrio AsteRx-i V integrated GNSS-inertial measurement unit (IMU) to produce the ground truth trajectory.

TABLE I
GNBs's Characteristics

gNB	Carrier frequency [MHz]	N_{ID}^{Cell}	Cellular provider
1	872	608	AT&T
2	632.55	398	T-Mobile

B. Signal Tracking Performance

Two gNBs were present in the environment whose positions were mapped prior to the experiment. In the tracking stage, the 5G signals from both gNBs were tracked for 100 seconds. Fig. 4 shows the tracking results of the two gNBs, while Fig. 5 shows the cumulative distribution function (CDF) of the errors.

C. Navigation Solution

An extended Kalman filter, as discussed in [18], was used to estimate the vehicle-mounted receiver's trajectory. The measurement variances were found to vary between 1.3 and 25.7 m. Fig. 6 shows the environment layout, location of gNBs, navigation solution of DLL-based and RL-based 5G, and receiver's ground truth. The proposed 5G RL approach achieved a position RMSE of 14.7 m compared to 20.6 m with a conventional DLL-based 5G receiver. It is worth noting that the receiver presented in [18] used additional reference signals (not used in this study), namely physical broadcast channel (PBCH) and its associated demodulation reference signal (DM-RS).

VI. Conclusion

This paper presented a proof-of-concept of the power of RL in learning multipath errors that corrupt the TOA estimate in a 5G opportunistic navigation receiver. The proposed approach is the first of its kind to not depend on a DLL, as it learns the errors from observed ACFs directly. The RL-CNN used inputs from the ACF to learn the errors in the code phase estimates. A ray tracing algorithm was used to produce high fidelity training data that could model the dynamics between the LOS component and the NLOS components. Experimental results in a multipath-rich environment were presented demonstrating that the proposed RL-CNN achieved a position RMSE of 14.7 m compared to 20.6 m achieved using the conventional DLL.

Acknowledgment

This work was supported in part by the Office of Naval Research (ONR) under Grant N00014-19-1-2511 and Grant N00014-19-1-2613, in part by the U.S. Department of Transportation (USDOT) under Grant 69A3552047138 for the CARMEN University Transportation Center (UTC), and in part under the financial assistance award 70NANB17H192 from U.S. Department of Commerce, National Institute of Standards and Technology (NIST). Map data copyrighted OpenStreetMap contributors and available from https://www.openstreetmap.org.

References

[1] A. Mannesson, M. Yaqoob, B. Bernhardsson, and F. Tufvesson, "Tightly coupled positioning and multipath radio channel tracking," *IEEE Transactions on Aerospace and Electronic Systems*, vol. 52, no. 4, pp. 1522–1535, August 2016.

[2] J. del Peral-Rosado, R. Estatuet-Castillo, J. Lopez-Salcedo, G. Seco-Granados, Z. Chaloupka, L. Ries, and J. Garcoa-Molina, "Evaluation of hybrid positioning scenarios for autonomous vehicle applications," in *Proceedings of ION International Technical Meeting Conference*, January 2017, pp. 2541–2553.

[3] T. Kang, H. Lee, and J. Seo, "TOA-based ranging method using CRS in LTE signals," *Journal of Advanced Navigation Technology*, vol. 23, no. 5, pp. 437–443, October 2019.

[4] K. Shamaei, J. Morales, and Z. Kassas, "A framework for navigation with LTE time-correlated pseudorange errors in multipath environments," in *Proceedings of IEEE Vehicular Technology Conference*, April 2019, pp. 1–6.

[5] X. Chen, Q. Wei, F. Wang, Z. Jun, S. Wu, and A. Men, "Super-resolution time of arrival estimation for a symbiotic FM radio data system," *IEEE Transactions on Broadcasting*, vol. 66, no. 4, pp. 847–856, December 2020.

[6] L. Xu and J. Rife, "Modeling multipath effects on frequency locked loops," in *Proceedings of ION International Technical Meeting*, 2020, pp. 698–712.

[7] H. Dun, C. Tiberius, and G. Janssen, "Positioning in a multipath channel using OFDM signals with carrier phase tracking," *IEEE Access*, vol. 8, pp. 13 011–13 028, 2020.

[8] P. Wang and Y. Morton, "Performance comparison of time-of-arrival estimation techniques for LTE signals in realistic multipath propagation channels," *NAVIGATION, Journal of the Institute of Navigation*, vol. 67, no. 4, pp. 691–712, December 2020.

[9] T. Kazaz, G. Janssen, J. Romme, and A. Van der Veen, "Delay estimation for ranging and localization using multiband channel state information," *IEEE Transactions on Wireless Communications*, pp. 1–16, September 2021.

[10] C. Jin, I. Bajaj, K. Zhao, W. Tay, and K. Ling, "5G positioning using code-phase timing recovery," in *Proceedings of IEEE Wireless Communications and Networking Conference*, 2021, pp. 1–7.

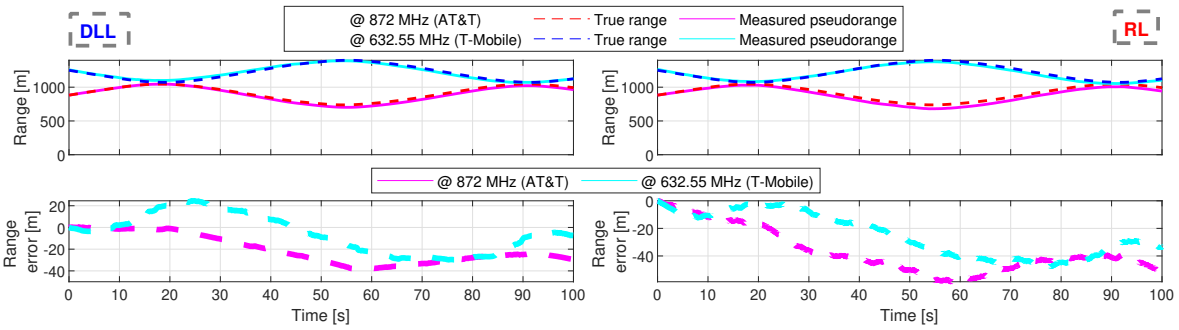

Fig. 4. Cellular 5G signal tracking results of the two gNBs for both DLL and RL approaches showing: (i) pseudorange estimate in solid lines versus true range in dashed lines after removing the initial bias and (ii) range errors.

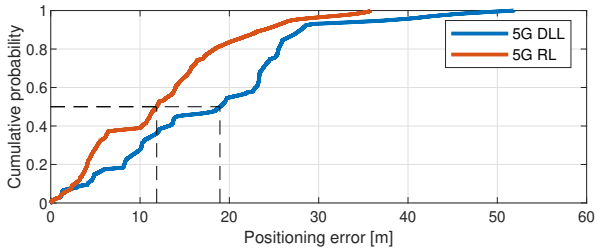

Fig. 5. CDF of positioning errors for DLL-based and RL-based approaches.

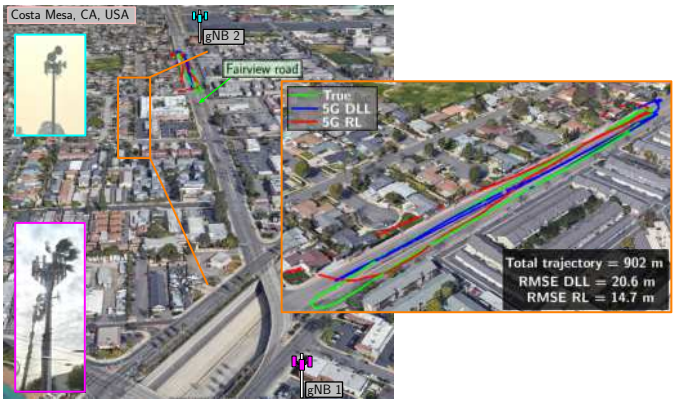

Fig. 6. 5G gNBs' locations and traversed trajectory: true (white), DLL-based estimate (blue), and RL-based estimate (red). Image: Google Earth.

[11] N. Souli, P. Kolios, and G. Ellinas, "Online relative positioning of autonomous vehicles using signals of opportunity," *IEEE Transactions on Intelligent Vehicles*, pp. 1–1, 2021.

[12] K. Shamaei and Z. Kassas, "Receiver design and time of arrival estimation for opportunistic localization with 5G signals," *IEEE Transactions on Wireless Communications*, vol. 20, no. 7, pp. 4716–4731, 2021.

[13] I. Lapin, G. Seco-Granados, O. Renaudin, F. Zanier, and L. Ries, "Joint delay and phase discriminator based on ESPRIT for 5G NR positioning," *IEEE Access*, vol. 9, pp. 126 550–126 563, 2021.

[14] A. Abdallah, J. Khalife, and Z. Kassas, "Experimental characterization of received 5G signals carrier-to-noise ratio in indoor and urban environments," in *Proceedings of IEEE Vehicular Technology Conference*, April 2021, pp. 1–5.

[15] A. Shahmansoori, G. Garcia, G. Destino, G. Seco-Granados, and H. Wymeersch, "Position and orientation estimation through millimeter-wave MIMO in 5G systems," *IEEE Transactions on Wireless Communications*, vol. 17, no. 3, March 2018.

[16] N. Garcia, H. Wymeersch, E. Larsson, A. Haimovich, and M. Coulon, "Direct localization for massive MIMO," *IEEE Transactions on Signal Processing*, vol. 65, no. 10, pp. 2475–2487, May 2017.

[17] K. Han, Y. Liu, Z. Deng, L. Yin, and L. Shi, "Direct positioning method of mixed far-field and near-field based on 5G massive MIMO system," *IEEE Access*, vol. 7, pp. 72 170–72 181, 2019.

[18] A. Abdallah, K. Shamaei, and Z. Kassas, "Assessing real 5G signals for opportunistic navigation," in *Proceedings of ION GNSS Conference*, 2020, pp. 2548–2559.

[19] Z. Kassas, A. Abdallah, and M. Orabi, "Carpe signum: seize the signal – opportunistic navigation with 5G," *Inside GNSS Magazine*, vol. 16, no. 1, pp. 52–57, 2021.

[20] A. Abdallah and Z. Kassas, "UAV navigation with 5G carrier phase measurements," in *Proceedings of ION GNSS Conference*, September 2021, pp. 3294–3306.

[21] D. Aloi and M. Sharawi, "High fidelity antenna model validation results of a GNSS multipath limiting antenna," *IEEE Transactions on Aerospace and Electronic Systems*, vol. 47, no. 1, pp. 3–14, January 2011.

[22] A. van Dierendonck, P. Fenton, and T. Ford, "Theory and performance of narrow correlator spacing in a GPS receiver," *NAVIGATION, Journal of the Institute of Navigation*, vol. 39, no. 3, pp. 265–283, September 1992.

[23] L. Garin, F. van Diggelen, and J. Rousseau, "Strobe and edge correlator multipath mitigation for code," in *Proceedings of ION International Technical Meeting*, January 1996, pp. 657–664.

[24] G. McGraw and M. Braasch, "GNSS multipath mitigation using gated and high resolution correlator concepts," in *Proceedings of ION National Technical Meeting*, January 1999, pp. 333–342.

[25] A. Abdallah and Z. Kassas, "Multipath mitigation via synthetic aperture beamforming for indoor and deep urban navigation," *IEEE Transactions on Vehicular Technology*, vol. 70, no. 9, pp. 8838–8853, September 2021.

[26] J. Gante, L. Sousa, and G. Falcao, "Dethroning GPS: Low-power accurate 5G positioning systems using machine learning," *IEEE Journal on Emerging and Selected Topics in Circuits and Systems*, vol. 10, no. 2, pp. 240–252, June 2020.

[27] M. Orabi, J. Khalife, A. Abdallah, Z. Kassas, and S. Saab, "A machine learning approach for GPS code phase estimation in multipath environments," in *Proceedings of IEEE/ION Position, Location, and Navigation Symposium*, April 2020, pp. 1224–1229.

[28] N. Sokhandan, N. Ziedan, A. Broumandan, and G. Lachapelle, "Context-aware adaptive multipath compensation based on channel pattern recognition for GNSS receivers," *NAVIGATION, Journal of the Institute of Navigation*, vol. 70, no. 5, pp. 944–962, September 2017.

[29] M. Orabi, A. Abdallah, J. Khalife, and Z. Kassas, "A machine learning multipath mitigation approach for opportunistic navigation with 5G signals," in *Proceedings of ION GNSS Conference*, September 2021, pp. 2895–2909.

[30] OpenStreetMap contributors, "Planet dump retrieved from https://planet.osm.org," https://www.openstreetmap.org, 2017.

[31] J. Danielson and D. Gesch, *Global multi-resolution terrain elevation data 2010 (GMTED2010)*. US Department of the Interior, US Geological Survey, 2011.

[32] "Matlab RF toolbox," https://www.mathworks.com/help/rf/index.html, 2021.

[33] P. Series, "Effects of building materials and structures on radiowave propagation above about 100 MHz," *Recommendation ITU-R*, pp. 2040–1, 2015.